

# Journal of Materials Chemistry C

Accepted Manuscript



This article can be cited before page numbers have been issued, to do this please use: H. Yu, C. Liu, Z. Yu, L. Zhang and J. Xiu, *J. Mater. Chem. C*, 2017, DOI: 10.1039/C6TC04732G.



This is an Accepted Manuscript, which has been through the Royal Society of Chemistry peer review process and has been accepted for publication.

Accepted Manuscripts are published online shortly after acceptance, before technical editing, formatting and proof reading. Using this free service, authors can make their results available to the community, in citable form, before we publish the edited article. We will replace this Accepted Manuscript with the edited and formatted Advance Article as soon as it is available.

You can find more information about Accepted Manuscripts in the [author guidelines](#).

Please note that technical editing may introduce minor changes to the text and/or graphics, which may alter content. The journal's standard [Terms & Conditions](#) and the ethical guidelines, outlined in our [author and reviewer resource centre](#), still apply. In no event shall the Royal Society of Chemistry be held responsible for any errors or omissions in this Accepted Manuscript or any consequences arising from the use of any information it contains.

## Effect of ancillary ligands on the properties of diphenylphosphoryl-substituted cationic Ir(III) complexes

Hongcui Yu, Chun Liu\*, Zhenni Yu, Liyan Zhang and Jinghai xiu\*

Received 00th January 20xx,  
Accepted 00th January 20xx

DOI: 10.1039/x0xx00000x

www.rsc.org/

A new class of diphenylphosphoryl-substituted cationic cyclometalated Ir(III) complexes  $[\text{Ir}(\text{POF}d\text{Fppy})_2(\text{N}^{\wedge}\text{N})]^+\text{PF}_6^-$  ( $d\text{Fppy}$  = 2-(2,4-difluorophenyl)pyridine) (**POF1-POF6**) with different  $\text{N}^{\wedge}\text{N}$  ancillary ligands have been synthesized and characterized. The influences of  $\text{N}^{\wedge}\text{N}$  ancillary ligands on the photophysical and electrochemical properties of the Ir(III) complexes have been investigated systematically. The results demonstrate that the photoluminescence quantum yields ( $\Phi_{\text{PL}}$ ) of the complexes are dependent on the  $\text{N}^{\wedge}\text{N}$  ancillary ligands. **POF1-POF3** equipped with phenanthroline or bipyridine ancillary ligands exhibit intense emission bands at 465–497 nm and high  $\Phi_{\text{PL}}$  in the range of 56–61% in  $\text{CH}_2\text{Cl}_2$ . The biimidazole-type complexes **POF4-POF6** exhibit an obvious substituent-effect on the photophysical and electrochemical properties. Although the emission spectra of **POF4** and **POF5** show similar fine structures, the  $\Phi_{\text{PL}}$  of **POF5** bearing two methyl groups at the biimidazole moiety is remarkably lower (5%) than that of **POF4** (45%, unmodified biimidazole). **POF6** bearing two phenyl groups at the biimidazole moiety exhibits a red-shift and weak emission band, and an extremely low  $\Phi_{\text{PL}}$  (<3%). However, the photoluminescence quantum yields of **POF5** and **POF6** (35% and 41% in EC film, 40% and 65% in neat film, respectively) in film increase effectively in comparison to those in solution. Cyclic voltammetry shows further that the structure of the ancillary ligand affects the redox properties. Density functional theory (DFT) and time-dependent DFT (TD-DFT) calculations were performed to provide insights into the electronic structures of **POF1-POF6**. **POF1** bearing a 1,10-phenanthroline moiety demonstrates the highest oxygen sensitivity.

### Introduction

Cyclometalated Ir(III) complexes are of special interest as promising phosphorescent materials and have been widely studied for their potential applications in organic light emitting diodes (OLEDs), light-emitting electrochemical cells (LEECs), biological and analytical probing, photocatalysis and so on.<sup>1–4</sup> The performances of these materials in such roles depend on their tunable emission colors and unique photoluminescence properties.<sup>5–8</sup>

Although a wide range of Ir(III) emitting materials from blue to the near-infrared have been reported so far, the number of highly efficient blue phosphorescent Ir(III) complexes are relatively limited. This is a challenging task because blue-emitting Ir(III) materials require a larger energy gap than other compounds and the photoluminescence quantum yield ( $\Phi_{\text{PL}}$ ) is often very low due to a significant increase in nonradiative decay rates.<sup>9–11</sup> The seminal sky-blue phosphorescent cyclometalated Ir(III) complex is iridium(III) bis[(4,6-difluorophenyl)-pyridinato- $N,C^2'$ ] picolinate (FIrpic),<sup>12</sup> which has proved to be an excellent phosphorescent material in OLEDs. Some popular strategies are adopted to tune the

emission to blue region and enhance  $\Phi_{\text{PL}}$  in Ir(III) complexes, which are attractive for both fundamental research and practical applications.<sup>13–19</sup>

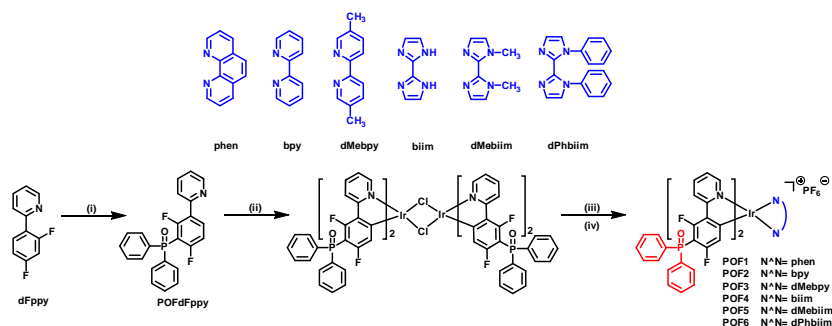
The diphenylphosphoryl ( $\text{Ph}_2\text{PO}$ ) moiety with its tetrahedral geometrical structure can suppress the molecular stacks and improve the electron-injecting and electron-transporting performances, which makes the  $\text{Ph}_2\text{PO}$  group widely used in designing new host materials.<sup>20–22</sup> At present, several Ir(III) complexes through tailoring the 2-phenylpyridine (ppy) type ligands with the  $\text{Ph}_2\text{PO}$  moiety have been developed.<sup>23–30</sup> However, blue phosphorescent diphenylphosphoryl-substituted Ir(III) complexes are rarely reported in the literature. In 2012, Yang and co-workers<sup>28</sup> reported a diphenylphosphoryl-substituted neutral Ir(III) complex  $\text{POFIrpic}$ , which has been successfully applied in the construction of efficient single-layer blue phosphorescent OLEDs. In 2014, Yun et al.<sup>29</sup> synthesized a complex  $\text{Ir}(\text{dppfm})_2\text{pic}$  by introducing a methyl group into the 4-position of pyridine in  $\text{POFIrpic}$ . As a blue phosphorescent emitter,  $\text{Ir}(\text{dppfm})_2\text{pic}$  was used in OLEDs, resulting in a maximum external quantum efficiency of 7.8%. Recently, Si et al.<sup>30</sup> investigated the structure-property relationship of several diphenylphosphoryl-substituted cationic Ir(III) complexes with different  $\text{N}^{\wedge}\text{N}$  ancillary ligands by the computational method. Their results revealed that different ancillary ligands affected not only the energy gap but also the  $\Phi_{\text{PL}}$ . However, to the best of our knowledge, a systematic experimental study on the

State Key Laboratory of Fine Chemicals, Dalian University of Technology, Linggong Road 2, Dalian 116024, China. E-mail: cliu@dlut.edu.cn; xiujh@dlut.edu.cn

†Electronic Supplementary Information (ESI) available: Experimental details and characterization of products. See DOI: 10.1039/x0xx00000x

effects of N^N ancillary ligands on the photophysical and electrochemical properties of the diphenylphosphoryl-substituted Ir(III) complexes has not been reported.

In this work, six diphenylphosphoryl-substituted cationic cyclometalated Ir(III) complexes  $[\text{Ir}(\text{POFdFppy})_2(\text{N}^{\wedge}\text{N})]^+\text{PF}_6^-$  (**POF1-POF6**) were designed and synthesized with different N^N ancillary ligands. The chemical structures and abbreviations for the N^N ancillary ligands, named phen, bpy, dMebpy, biim, dMebiim and dPhbiim, are illustrated in Scheme 1. **POF1-POF6** allow us to explore the effects of different N^N ancillary ligands on the photophysical and electrochemical properties of the corresponding Ir(III) complexes. In addition, the oxygen sensitivity of these Ir(III) complexes was also studied.



**Scheme 1** Chemical structures of ancillary ligands and synthetic routes of Ir(III) complexes **POF1-POF6**.

(i) LDA, ether,  $-78\text{ }^\circ\text{C}$ ,  $\text{N}_2$ , 1.5 h;  $\text{Ph}_2\text{PCl}$ , overnight, RT;  $\text{H}_2\text{O}_2$ ,  $\text{CH}_2\text{Cl}_2$ , 3 h. (ii)  $\text{IrCl}_3 \cdot 3\text{H}_2\text{O}$ ,  $\text{EtOCH}_2\text{CH}_2\text{OH}/\text{H}_2\text{O}$ , 3 : 1 (v/v),  $120\text{ }^\circ\text{C}$ ,  $\text{N}_2$ , 24 h. (iii) N^N ancillary ligand,  $\text{CH}_2\text{Cl}_2/\text{MeOH}$ , 2 : 1 (v/v),  $50\text{ }^\circ\text{C}$ ,  $\text{N}_2$ , 12 h. (iv)  $\text{KPF}_6$ , RT, 1.5 h.

### Photophysical properties

UV-vis absorption spectra of **POF1-POF6** in  $\text{CH}_2\text{Cl}_2$  at room temperature are presented in Fig. 1a and the corresponding photophysical data are given in Table 1. All complexes exhibit intense absorptions with high molar extinction coefficients ( $\epsilon = 4.63\text{--}7.64 \times 10^4\text{ M}^{-1}\text{ cm}^{-1}$ ) at high energy (230–260 nm), and the biimidazole-type complexes possess additional sharp, intense absorptions near 286 nm. The absorption bands at high energy are similar to those of the corresponding free ligands (see Fig. S1, ESI) and are assigned to spin-allowed intraligand ( $^1\pi\text{--}\pi^*$ ) transitions. The weaker absorption bands (inset of Fig. 1(a)) are assigned to mixing among metal-to-ligand and ligand-to-ligand charge transfer (MLCT/LLCT) together with ligand-centered ( $^3\pi\text{--}\pi^*$ ) transitions.<sup>31, 32</sup> **POF1** exhibits the highest molar extinction coefficient, which might be due to the larger conjugation degree of phen compared to other N^N ancillary ligands (see Fig. S1, ESI).<sup>33-35</sup>

At room temperature, the emission spectra of **POF1-POF6** in  $\text{CH}_2\text{Cl}_2$  are shown in Fig. 1b. **POF1-POF3** emit greenish-blue colors at 465–497 nm with high  $\Phi_{\text{PL}}$  of 56%, 61% and 58%, respectively.  $[\text{Ir}(\text{POFdFppy})_2(\text{phen})]^+\text{PF}_6^-$  (**POF1**) ( $\lambda_{\text{max}} = 470\text{ nm}$ ) with a phen ancillary ligand emits a greenish-blue color, which is blue-shifted relative to  $[\text{Ir}(\text{POFdFppy})_2(\text{bpy})]^+\text{PF}_6^-$  (**POF2**) ( $\lambda_{\text{max}} = 493\text{ nm}$ ). Introducing  $-\text{CH}_3$  into the 5,5'-position of 2,2'-bipyridine, the emission spectrum of  $[\text{Ir}(\text{POFdFppy})_2(\text{dMebpy})]^+\text{PF}_6^-$  (**POF3**) ( $\lambda_{\text{max}} = 465\text{ nm}$ ) becomes narrower and more structured compared with that of **POF2**.

## Results and discussion

### Synthesis and characterization

Chemical structures and the synthetic protocols of the cationic cyclometalated Ir(III) complexes **POF1-POF6** are shown in Scheme 1. The ligands used in this work were synthesized according to the reported procedures (see ESI). All of the Ir(III) complexes were synthesized in a three-step route: cyclometalated Ir(III)  $\mu$ -chloro-bridged dimers were first obtained, followed by treatment with the corresponding N^N ancillary ligand, and then a counterion exchange reaction from  $\text{Cl}^-$  to  $\text{PF}_6^-$ . The corresponding characterization data for all Ir(III) complexes are presented in the experimental section.

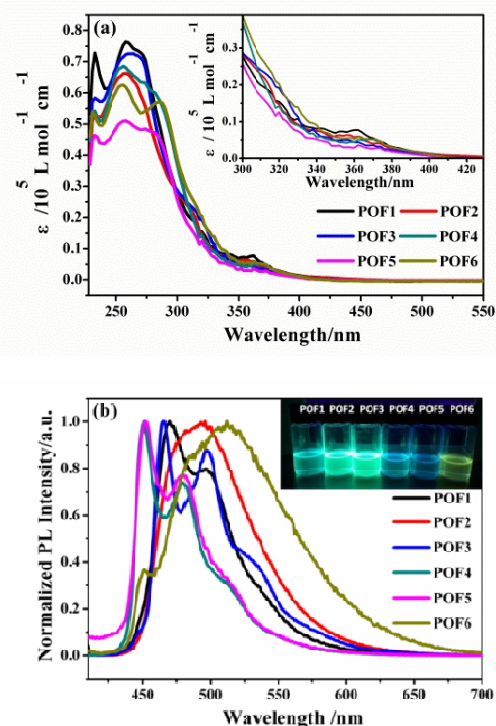


**Fig. 1** Absorption (a) and emission (b) spectra of Ir(III) complexes **POF1-POF6** in  $\text{CH}_2\text{Cl}_2$  ( $1.0 \times 10^{-5}\text{ M}$ ) at room temperature. The inset in (a) shows the magnified spectra from 300 to 430 nm. The inset in (b) shows the emission photographs in  $\text{CH}_2\text{Cl}_2$  (excited at 365 nm by a UV lamp).

When a biim ancillary ligand is used,  $[\text{Ir}(\text{POFdBpy})_2(\text{biim})]^+\text{PF}_6^-$  (**POF4**) ( $\lambda_{\text{max}} = 451 \text{ nm}$ ) shows the most obviously blue-shifted emission spectrum compared to other complexes. The emission spectrum of **POF4** in 2-MeTHF at 77K exhibits a little rigidochromic blue-shift (5 nm) compared with that in  $\text{CH}_2\text{Cl}_2$  at room temperature (see Fig. S3, ESI). **POF4** with a  $\Phi_{\text{PL}}$  of 45% gives a blue-shift of approximately 13 nm versus the emission of the unsubstituted complex<sup>36</sup>  $[\text{Ir}(\text{dFppy})_2(\text{biim})]^+\text{PF}_6^-$  ( $\lambda_{\text{max}} = 464 \text{ nm}$ ,  $\Phi_{\text{PL}} = 20\%$  in MeOH). The results demonstrate an excellent combination of the 2,2'-biimidazole ancillary ligand and the diphenylphosphoryl-substituted cyclometalating ligand for the construction of a blue cationic cyclometalated Ir(III) complex with a relatively high  $\Phi_{\text{PL}}$ .

Instead of the ancillary ligand biim with dMebiim,  $[\text{Ir}(\text{POFdBpy})_2(\text{dMebiim})]^+\text{PF}_6^-$  (**POF5**) ( $\lambda_{\text{max}} = 452 \text{ nm}$ ) has similar structured emission with **POF4**. When a dPhbiim is used as the ancillary ligand, the red-shifted emission spectrum of  $[\text{Ir}(\text{POFdBpy})_2(\text{dPhbiim})]^+\text{PF}_6^-$  (**POF6**) becomes a broader and almost unstructured shape characteristic. This may be attributed to the different nature of the emissive excited state, which contains much more character of  $^3\text{MLCT}/^3\text{LLCT}$  than those of other complexes. The assignments of the transitions are further supported by theoretical calculations (see theoretical calculations section). Additionally, the use of either dMebiim or dPhbiim as the ancillary ligand induces a significant decrease in  $\Phi_{\text{PL}}$  of the resulting Ir(III) complexes **POF5** and **POF6**. The  $\Phi_{\text{PL}}$  of **POF6** in  $\text{CH}_2\text{Cl}_2$  is extremely low (Table 1,  $\Phi_{\text{PL}} < 3\%$ , even lower than that of **POF5**,  $\Phi_{\text{PL}} = 5\%$ ), which might be due to the undesired twisting of the methyl or phenyl group on the dMebiim or dPhbiim ancillary ligand, resulting in increased nonradiative decay pathways.<sup>37</sup> It is clear that, introduction of the methyl or phenyl group into the 1 and 1' positions of biimidazole ligand has a negative effect on the  $\Phi_{\text{PL}}$  of the corresponding complexes **POF5** and **POF6** in  $\text{CH}_2\text{Cl}_2$ .

The phosphorescent lifetimes ( $\tau$ ) of **POF1-POF4** in  $\text{CH}_2\text{Cl}_2$  were measured to be 2.66-1.32  $\mu\text{s}$  at room temperature (Table 1, the phosphorescence decay profiles of the Ir(III) complexes are provided in Fig. S4, ESI). However, the  $\tau$  values for **POF5** and **POF6** drop significantly ( $\leq 0.37 \mu\text{s}$ ), which may result from large nonradiative decay caused by the activated bond rotation of dMebiim and dPhbiim ancillary ligands in **POF5** and **POF6**. Thus, the substituent effect of ancillary ligand plays an important role in tuning the photoluminescence properties of the Ir(III) complexes. The radiative decay rate ( $k_r$ ) and nonradiative decay rate ( $k_{\text{nr}}$ ) of the complexes in  $\text{CH}_2\text{Cl}_2$  were calculated (Table 1). The brightest complex **POF2** has a  $k_r$  of  $4.62 \times 10^5 \text{ s}^{-1}$ . It is notable that the large difference in  $\Phi_{\text{PL}}$  between **POF4** and **POF5** is owing to the distinctively different nonradiative decay rate constants,  $k_{\text{nr}}$ , of  $3.31 \times 10^5 \text{ s}^{-1}$  for **POF4** and  $25.68 \times 10^5 \text{ s}^{-1}$  for **POF5**. Due to a very low emission, the data for **POF6** could not be measured. It is obvious that a large  $k_r$  and a small  $k_{\text{nr}}$  would be favorable for a high  $\Phi_{\text{PL}}$ .

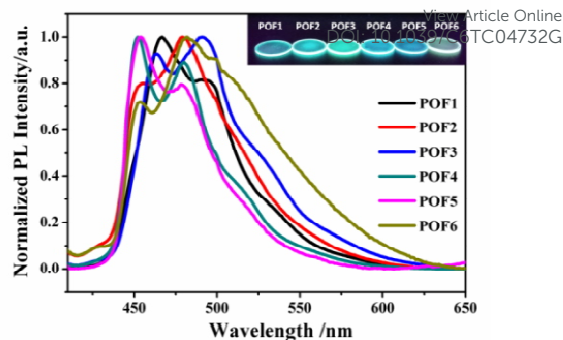


Fig. 2 Emission spectra of Ir(III) complexes **POF1-POF6** in 0.5 wt% doped EC film at room temperature. The inset shows the emission photographs in EC film (excited at 365 nm by a UV lamp).

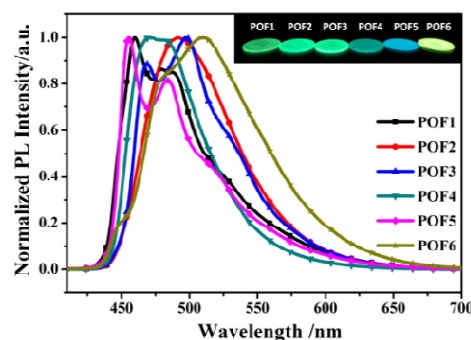


Fig. 3 Emission spectra of Ir(III) complexes **POF1-POF6** in neat film at room temperature. The inset shows the emission photographs in neat film (excited at 365 nm by a UV lamp).

The emission spectra and photoluminescence quantum yields of **POF1-POF6** in neat and doped (0.5 wt% in EC) films were also measured. The pertinent data are summarized in Table 1. As shown in Fig. 2, the emission maxima of **POF1-POF6** in EC film are ranging from 452 to 493 nm. Their absolute photoluminescence quantum yields in EC film are 61%, 58%, 64%, 45%, 35% and 41%, respectively. Compared with the emission spectra in solutions, the emission spectra of **POF2** and **POF6** in EC film exhibit blue-shift (see Fig. S1, ESI) due to the rigidochromic effect.<sup>38, 39</sup> The neat film emission maxima are in the range of 455-510 nm for **POF1-POF6** with absolute photoluminescence quantum yields of 57%, 63%, 60%, 33%, 40% and 65%, respectively (Fig. 3 and Table 1). In neat film, the emission spectra of all complexes except **POF4** are almost identical to those in solutions (see Fig. S1, ESI). The complex **POF4** with a biim ancillary ligand exhibits a red-shifted emission accompanied by a reduced absolute photoluminescence quantum yield compared with that in EC film, most probably due to intermolecular interactions.<sup>40, 41</sup> **POF1-POF3** in the solid states exhibit phosphorescence behaviors similar to those in solutions, indicating that the sterically bulky diphenylphosphoryl group might work effectively in suppressing the intermolecular interactions and excited-state self-quenching of the complexes from solution to solid state.<sup>28, 42</sup> Very interestingly, **POF5** and **POF6** exhibit bright light in the solid state under UV light, differing from their weak phosphorescence in the dilute solutions. The most

probable reason is that the intramolecular motion is restricted in the solid state, which is considered as the main cause of aggregation-induced phosphorescent emission enhancement properties.<sup>43-45</sup> The emission spectra of **POF6** in water/CH<sub>3</sub>CN mixtures with different water content (0-90%) were detected (see Fig. S6, ESI). The intensity of emission increased gradually

with the variation of the proportion of H<sub>2</sub>O. Since **POF6** is insoluble in water, it could gradually aggregate upon the addition of water, showing an aggregation-induced phosphorescent emission enhancement property.

**Table 1** Photophysical data of **POF1-POF6**.

Complex	$\lambda_{\text{abs}}^a$ (nm)	$\lambda_{\text{em}}^b$ (nm)	$\Phi_{\text{EC}}^c$	$\Phi_{\text{neat}}^d$	In CH <sub>2</sub> Cl <sub>2</sub>			
					$\Phi_{\text{solution}}^e$	$\tau^e$ ( $\mu\text{s}$ )	$k_r^e$ ( $10^5 \text{ s}^{-1}$ )	$k_{\text{nr}}^e$ ( $10^5 \text{ s}^{-1}$ )
<b>POF1</b>	232(7.28), 258(7.64), 362(0.77)	<b>470,496</b> (CH <sub>2</sub> Cl <sub>2</sub> )	0.61	0.57	0.56	2.40	2.33	1.83
		<b>470,493</b> (CH <sub>3</sub> CN)						
		<b>467,493</b> (EC film)						
		<b>459,479</b> (neat film)						
<b>POF2</b>	232(5.42), 256(6.86), 368(0.52)	<b>493</b> (CH <sub>2</sub> Cl <sub>2</sub> )	0.58	0.63	0.61	1.32	4.62	2.95
		<b>492</b> (CH <sub>3</sub> CN)						
		<b>455,479</b> (EC film)						
		<b>492</b> (neat film)						
<b>POF3</b>	232(4.63), 258(5.11), 362(0.36)	<b>465,496</b> (CH <sub>2</sub> Cl <sub>2</sub> )	0.64	0.60	0.58	2.66	2.18	1.58
		<b>463,491</b> (CH <sub>3</sub> CN)						
		<b>463,491</b> (EC film)						
		<b>468,497</b> (neat film)						
<b>POF4</b>	230(5.40), 255(6.25), 286(5.71), 362(0.59)	<b>451,479</b> (CH <sub>2</sub> Cl <sub>2</sub> )	0.45	0.33	0.45	1.66	2.71	3.31
		<b>453,480</b> (CH <sub>3</sub> CN)						
		<b>452,480</b> (EC film)						
		<b>470,482</b> (neat film)						
<b>POF5</b>	230(5.40), 255(6.25), 286(5.71), 362(0.59)	<b>452,480</b> (CH <sub>2</sub> Cl <sub>2</sub> )	0.35	0.40	0.05	0.37	1.35	25.68
		<b>452,479</b> (CH <sub>3</sub> CN)						
		<b>454,478</b> (EC film)						
		<b>455,484</b> (neat film)						
<b>POF6</b>	230(5.40), 255(6.25), 286(5.71), 362(0.59)	<b>451,512</b> (CH <sub>2</sub> Cl <sub>2</sub> )	0.41	0.65	< 0.03	<i>f</i>	<i>f</i>	<i>f</i>
		<b>452,516</b> (CH <sub>3</sub> CN)						
		<b>453,482</b> (EC film)						
		<b>483,510</b> (neat film)						

<sup>a</sup> Measured in CH<sub>2</sub>Cl<sub>2</sub> at a concentration of 10<sup>-5</sup> M and extinction coefficients (10<sup>4</sup> M<sup>-1</sup>cm<sup>-1</sup>) are shown in parentheses. <sup>b</sup> The emission maxima are the values in bold style ( $\lambda_{\text{exc}} = 360$  nm). <sup>c</sup> Measured in 0.5 wt% doped EC film by the absolute method using an integrating sphere ( $\lambda_{\text{exc}} = 360$  nm). <sup>d</sup> Measured in neat film by the absolute method using an integrating sphere ( $\lambda_{\text{exc}} = 360$  nm). <sup>e</sup> The quantum yields ( $\Phi_{\text{solution}}$ ) in deoxygenated CH<sub>2</sub>Cl<sub>2</sub> were measured with [Ir(ppy)<sub>2</sub>(acac)] ( $\Phi_{\text{PL}} = 0.34$ ) as a standard, radiative and nonradiative decay rates of  $k_r$  and  $k_{\text{nr}}$  were calculated from  $k_r = \Phi_{\text{PL}} \times \tau^{-1}$ ,  $k_{\text{nr}} = \tau^{-1} - k_r$ . <sup>f</sup> Data not was not measured due to a very low emission. All measured at ambient temperature.

### Electrochemical Properties

The electrochemical properties of **POF1-POF6** were measured by cyclic voltammetry (CV) in CH<sub>2</sub>Cl<sub>2</sub> (the cyclic voltammograms of **POF1-POF6** see Fig. S4, ESI) and the corresponding data are presented in Table 2. The CVs of **POF1-POF3** display similar onset oxidation potentials at approximately 1.87 V and they are more anodic than those of **POF4-POF6** (1.68, 1.64, and 1.58 V, respectively). **POF1** and **POF2** show much less negative onset reduction potentials (-1.25 V for **POF1** and -1.22 V for **POF2**), which indicates their lower LUMO energy levels. Introducing the methyl substituent at the 5,5'-position of 2,2'-bipyridine for **POF3** makes the reduction process shift to a more cathodic potential at -1.38 V. The biimidazole-type complexes **POF4-POF6** show more negative reduction potentials relative to **POF1-POF3** because the biimidazole moiety is more electron-rich than phenanthroline and

bipyridine. Additionally, **POF4** and **POF5** have similar redox potentials and exhibit larger redox gaps than others. The redox potential of **POF6** is affected by the dPhbiim ancillary ligand, and **POF6** has a lower redox gap than that of **POF4**. Thus, it is clear that the structure of the ancillary ligand affects the electrochemical properties of the corresponding Ir(III) complexes.

The measured onset oxidation and reduction potentials of each Ir(III) complex were used to calculate the HOMO and LUMO levels, respectively. As listed in Table 2, the energy gaps ( $E_g$ ) between the HOMO and LUMO levels of **POF1-POF6** are 3.12, 3.10, 3.23, 3.53, 3.52 and 3.30 eV, respectively, which agree well with the observed greenish-blue to blue emission spectra of these complexes.

**Table 2** Electrochemical data of **POF1-POF6**.

Complex	$E_{ox}^{onset^a}$ [V]	$E_{red}^{onset^a}$ [V]	$E_g^b$ [eV]	HOMO <sup>c</sup> [eV]	LUMO <sup>c</sup> [eV]
<b>POF1</b>	1.87	-1.25	3.12	-6.27	-3.15
<b>POF2</b>	1.88	-1.22	3.10	-6.28	-3.18
<b>POF3</b>	1.85	-1.38	3.23	-6.25	-3.02
<b>POF4</b>	1.68	-1.85	3.53	-6.08	-2.55
<b>POF5</b>	1.64	-1.88	3.52	-6.04	-2.52
<b>POF6</b>	1.58	-1.72	3.30	-5.98	-2.68

<sup>a</sup> 0.1 M [Bu<sub>4</sub>N]PF<sub>6</sub> in CH<sub>2</sub>Cl<sub>2</sub>, scan rate 100 mV s<sup>-1</sup>, measured using saturated calomel electrode (SCE) as the standard. <sup>b</sup>  $E_g = E_{LUMO} - E_{HOMO}$ . <sup>c</sup>  $E_{HOMO}(eV) = -e(4.4 + E_{ox}^{onset})$ ,  $E_{LUMO}(eV) = -e(4.4 + E_{red}^{onset})$ , HOMO and LUMO denote highest-occupied molecular orbital and lowest-unoccupied molecular orbital, respectively.

### Theoretical calculations

The electronic structures of **POF1-POF6** were investigated by density functional theory (DFT) and time-dependent DFT (TD-DFT) calculations. As shown in Fig. 4, **POF1-POF3** present similar molecular orbital topologies, the HOMOs of **POF1-POF3** reside on the iridium center and ppy of the cyclometalating ligands, while the LUMOs reside on the ancillary ligands. The LUMOs appear at similar energies for **POF1** (-2.80 eV) and **POF2** (-2.84 eV), justifying the almost identical values recorded for the reduction potential of both complexes (-1.25 and -1.22 V, Table 2). The LUMO of **POF3** (-2.72 eV) is slightly destabilized by the electron-donating effect of the -CH<sub>3</sub> substituent in accord with a more cathodic

reduction potential measured by CV (-1.38 V, Table 2). The replacement of the phen- or bpy-type ligand by a biimidazole-type ligand results in destabilization of both the HOMO and LUMO energies with a increase in the overall energy gap, which is also supported by experimental results (Table 2). Different from **POF1-POF3**, the HOMOs of **POF4-POF6** are predominantly at the ppy of the cyclometalating ligand, iridium atom and biimidazole moieties of ancillary ligand. The LUMOs of **POF4** and **POF5** are mainly localized on the ppy of cyclometalating ligand and biimidazole of ancillary ligand. Substitution of 2,2'-biimidazole by -CH<sub>3</sub> the complex **POF5** shows nearly the same LUMO and HOMO levels relative to **POF4** (Fig. 4), in accord with the experimental results (Table 2). However, the LUMO of **POF6** is mainly localized at the biimidazole moieties of ancillary ligand, and also partially at the phenyl rings of the ancillary ligand. Compared with **POF4** and **POF5**, there is a decrease in the HOMO-LUMO energy gap for **POF6**, which is in good agreement with the experimental results (Table 2).

The vertical excitation energies and molecular orbitals involved in the excitations for the lowest energy triplet state (T<sub>1</sub>) are summarized in Table 3 (Electron density maps of the frontier molecular orbital of **POF1-POF6** at the ground state optimized geometries, see Fig. S7, ESI). Besides the predominant characters of <sup>3</sup>MLCT and <sup>3</sup>LLCT, the T<sub>1</sub> states of **POF1-POF3** have different degrees of <sup>3</sup>LC character. **POF4** and **POF5** have the predominant <sup>3</sup>LC nature of the T<sub>1</sub> state, which explains the fine structures of emission spectra. However, the emitting excited state of **POF6** involves much more <sup>3</sup>MLCT/<sup>3</sup>LLCT character, which can explain its broad unstructured emission band.

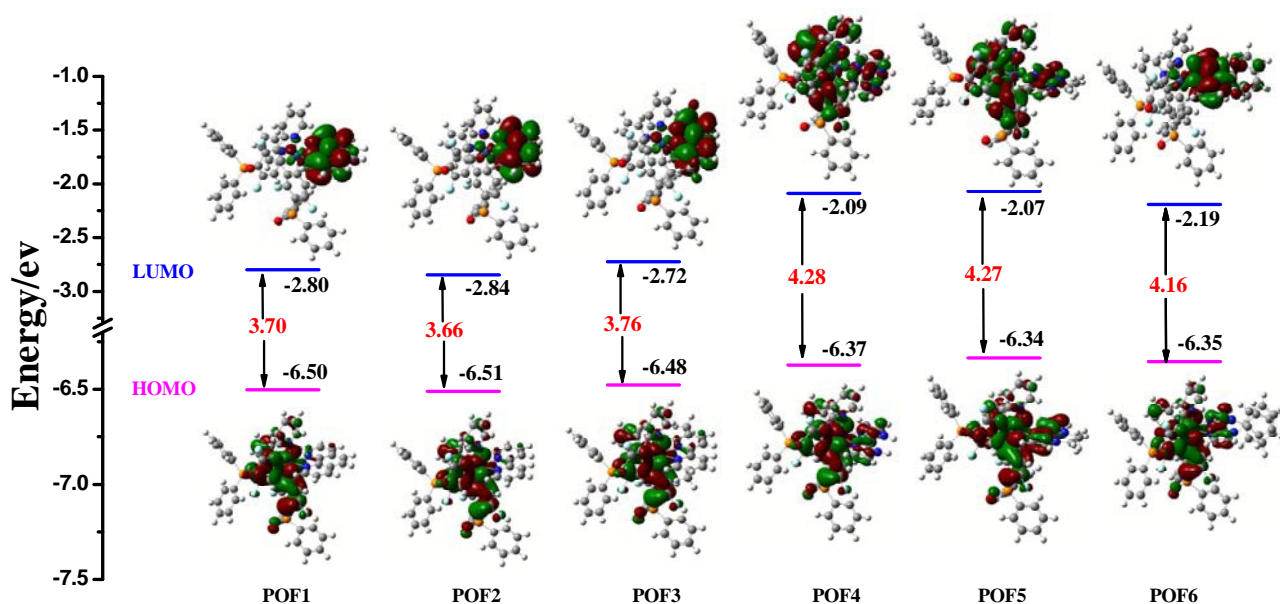


**Fig. 4** Calculated frontier molecular orbital energy levels together with the electron density distributions for **POF1-POF6**.

**Table 3** Calculated triplet states of **POF1-POF6** by a TD-DFT approach.

Complex	State	$E^a$ (eV)	Composition <sup>b</sup>	CI <sup>c</sup>	Character
<b>POF1</b>	$T_1$	2.83	H-13 $\rightarrow$ L+1	0.3233	LC
			H-4 $\rightarrow$ L+1	0.2735	LC/MLCT/LLCT
			H $\rightarrow$ L	0.2323	MLCT/LLCT
<b>POF2</b>	$T_1$	2.81	H $\rightarrow$ L	0.5663	MLCT/LLCT
			H-14 $\rightarrow$ L	0.1989	LC
			H-1 $\rightarrow$ L	0.1556	MLCT/LLCT
<b>POF3</b>	$T_1$	2.83	H $\rightarrow$ L	0.3972	MLCT/LLCT
			H-13 $\rightarrow$ L	0.3639	LC
			H-4 $\rightarrow$ L	0.3335	LC/MLCT/LLCT
<b>POF4</b>	$T_1$	2.95	H $\rightarrow$ L	0.4624	LC
			H-4 $\rightarrow$ L	0.2282	LC/LLCT
			H $\rightarrow$ L+1	0.2071	LC/MLCT
<b>POF5</b>	$T_1$	2.92	H-2 $\rightarrow$ L+1	0.4958	LC
			H $\rightarrow$ L+1	0.3593	LC/MLCT/LLCT
			H-2 $\rightarrow$ L	0.2185	LC/LLCT
<b>POF6</b>	$T_1$	2.87	H-2 $\rightarrow$ L	0.5310	LC/MLCT
			H $\rightarrow$ L	0.3804	MLCT/LLCT
			H-3 $\rightarrow$ L	0.1757	LLCT

<sup>a</sup> Only the selected low-lying excited states are presented. <sup>b</sup> Only the main configurations are presented. H and L denote HOMO and LUMO, respectively. <sup>c</sup> The Configuration-interaction (CI) coefficients are in absolute values. Oscillator strengths are zero because of the neglect of spin-orbit coupling in the TD-DFT calculations.

### Oxygen sensitivity properties

Cyclometalated Ir(III) complexes are an important class of probes for oxygen sensing.<sup>46</sup> A new family of cyclometalated Ir(III) complexes with good oxygen sensing properties have been reported.<sup>47-50</sup> So far, many cyclometalated Ir(III) oxygen-sensitive probes (OSPs) used for oxygen sensing are orange or green emitters, while greenish-blue to blue phosphorescent Ir(III) complexes as the OSPs are rarely reported.<sup>16</sup> Therefore, it is attractive for developing blue OSPs, which may provide a possibility to improve the efficiency of the sensors in the entire region of the visible spectrum. In this study, the oxygen sensitivity of **POF1-POF6** as greenish-blue to blue Ir(III) emitters were evaluated. The ethylcellulose (EC) with a high oxygen permeability coefficient was used to immobilize the Ir(III) complexes<sup>51</sup> and the corresponding data were fitted by a two-site model (Table S1, ESI)<sup>52-54</sup>. The  $I_0/I_{100}$  ratio ( $I_0$  and  $I_{100}$  represent the detected phosphorescent intensities from a film exposed to 100% N<sub>2</sub> and 100% O<sub>2</sub>, respectively) can be used to evaluate the oxygen sensitivity.

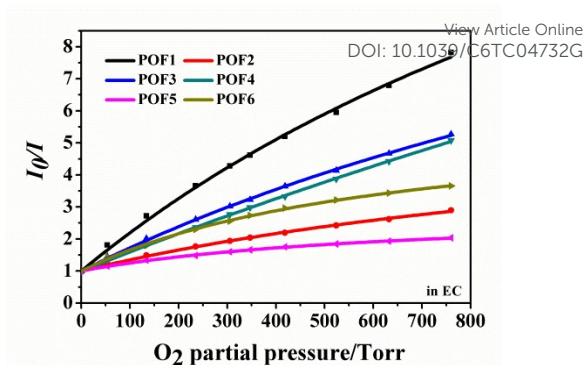


**Fig. 5** Stern-Volmer plots for oxygen sensing films of **POF1-POF6** (0.5 wt%) immobilized in EC (intensity ratios  $I_0/I$  versus O<sub>2</sub> partial pressure).

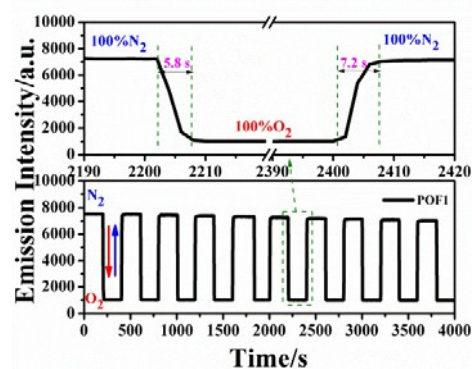


**Fig. 6** Response time and reversibility of **POF1** (0.5 wt%) immobilized in EC when cycling from 100% N<sub>2</sub> to 100% O<sub>2</sub> atmosphere.

The  $I_0/I_{100}$  values of these Ir(III) complexes immobilized in EC films are 7.7, 2.8, 5.2, 5.0, 2.0 and 3.6 respectively. Stern-Volmer plots are shown in Fig. 5. **POF1** bearing a phen ancillary ligand supported in EC exhibits the highest oxygen sensitivity. The oxygen sensing film of **POF1** demonstrates good reproducibility while oxygenated and deoxygenated gases were switched for 4000 s (Fig. 6). Additionally, fast response time (ca. 5.8 s for switching from N<sub>2</sub> to O<sub>2</sub>) and recovery time (ca. 7.2 s for switching from O<sub>2</sub> to N<sub>2</sub>) were obtained. Other Ir(III) complexes relatively less sensitive to quenching by O<sub>2</sub> can be envisioned for some systems such as water splitting and OLED display.

### Conclusions

In summary, a series of new diphenylphosphoryl-substituted cationic cyclometalated Ir(III) complexes [Ir(POFdFppy)<sub>2</sub>(N<sup>^</sup>N)]<sup>+</sup>PF<sub>6</sub><sup>-</sup> with different N<sup>^</sup>N ancillary ligands have been designed and synthesized. Both of experimental and theoretical results demonstrate that the structures of ancillary ligands strongly affect the photophysical and electrochemical properties of the corresponding Ir(III) complexes. In this study, all Ir(III) complexes show emission from the greenish-blue to blue at room temperature. The electron-rich 2,2'-biimidazole (biim) ancillary ligand is found to be the most useful one for constructing a blue Ir(III) complex **POF4**, compared with phen- and bpy-type Ir(III) complexes **POF1-POF3**. The complexes **POF1-POF4** show high  $\Phi_{PL}$  both in

solution and in solid state. In contrast to **POF4**, **POF5** and **POF6** with the electron-donating substituents of methyl or phenyl at the biim ancillary ligand show a significant decrease in  $\Phi_{\text{PL}}$  in  $\text{CH}_2\text{Cl}_2$ . **POF5** and **POF6** exhibit much higher  $\Phi_{\text{PL}}$  in solid state than those in solution. Electrochemical measurements showed that the redox potentials of phen- and bpy-type complexes **POF1-POF3** are shifted anodically compared to those of the biimidazole-type complexes **POF4-POF6**. When immobilized in ethyl cellulose film, **POF1** bearing a phen ancillary ligand exhibits the highest oxygen sensitivity. The above results show clearly that it is possible to tune the emission color,  $\Phi_{\text{PL}}$  and oxygen sensitivity properties of the Ir(III) complexes by the N^N ancillary ligands.

## Experimental

### Materials and instruments

All starting materials were purchased from commercial suppliers and used without further purification.  $^1\text{H}$  NMR and  $^{13}\text{C}$  NMR spectra were recorded on a 400 MHz Varian Unity Inova spectrophotometer. Mass spectra were recorded with a MALDI micro MX spectrometer. Elemental analyses for C, H, and N were performed on an Elementar-vario EL III elemental analyzer. UV-Vis absorption spectra were recorded on a Lambda 750s spectrophotometer. Emission spectra were recorded with a HITACHI F-7000 spectrofluorimeter ( $\lambda_{\text{exc}} = 360$  nm). Phosphorescence lifetimes were measured on an Edinburgh FLS920 spectrometer. An Oxford OptistatDN-V cryostat instrument equipped with an intelligent temperature controller and liquid nitrogen was used for data recorded at 77 K. Photoluminescence quantum yields ( $\Phi_{\text{PL}}$ ) were measured relative to  $[\text{Ir}(\text{ppy})_2(\text{acac})]$  ( $\Phi_{\text{PL}} = 0.34$  in  $\text{CH}_2\text{Cl}_2$ , under deoxygenated conditions). Solid state  $\Phi_{\text{PL}}$  values were measured using an absolute PL quantum yield measurement system (C11347-11, Hamamatsu Photonics K.K.). Cyclic voltammograms of the Ir(III) complexes were recorded on an electrochemical workstation (BAS100B/W, USA) at room temperature in a 0.1 M  $[\text{Bu}_4\text{N}]\text{PF}_6$  solution under argon conditions. Phosphorescent intensity response of sensing films of the Ir(III) complexes were recorded with a F-7000 spectrofluorimeter. The structures of the Ir(III) complexes were optimized using density functional theory (DFT) with the B3LYP functional and 6-31G(d)/LanL2DZ basis set. The LanL2DZ basis set was used to treat the iridium atom, whereas the 6-31G(d) basis set was used to treat all other atoms. All calculations were performed with the Gaussian 09 software package.<sup>55</sup>  $\text{CH}_2\text{Cl}_2$  was used as the solvent for the calculations (CPCM model).

### Synthesis

**Synthesis of C^N cyclometalating ligand and N^N ancillary ligands.** The different C^N cyclometalating ligand and N^N ancillary ligands were synthesized by previously reported method (see ESI).

**Synthesis of the Ir(III) complexes POF1-POF6.**  $\text{IrCl}_3 \cdot 3\text{H}_2\text{O}$  (0.5 mmol) and 2.5 equiv. of cyclometalating ligand were dissolved

in a mixture of 2-ethoxyethanol (15 mL) and water (5 mL) and refluxed at 120 °C under nitrogen for 24 h. After cooling, the solid precipitate was collected, washed with water and EtOH. Without any further purification, the dimeric Ir(III) complex reacted with 3.0 equiv. desired ancillary ligand in a mixture of dichloromethane (10 mL) and methanol (5 mL) at 50 °C under nitrogen for 12 h. The reaction mixture was cooled to room temperature and an aqueous solution of  $\text{KPF}_6$  was added to afford the crude product. The resulting solid was filtered, further purified by column chromatography over silica using  $\text{CH}_2\text{Cl}_2$ : petroleum ether (1:1) as eluent to provide the desired Ir(III) complexes.

**POF1:** Yield 52%, yellow solid;  $^1\text{H}$  NMR (400 MHz,  $\text{DMSO}-d_6$ )  $\delta$  8.97 (d,  $J = 8.3$  Hz, 2H), 8.42 (s, 2H), 8.38 – 8.33 (m, 2H), 8.12 (dd,  $J = 8.3, 5.1$  Hz, 2H), 8.06 (d,  $J = 8.8$  Hz, 2H), 7.89 (t,  $J = 8.2$  Hz, 2H), 7.83 – 7.75 (m, 8H), 7.63 – 7.52 (m, 14H), 7.06 (t,  $J = 6.7$  Hz, 2H), 5.82 (dd,  $J = 9.6, 3.6$  Hz, 2H).  $^{13}\text{C}$  NMR (100 MHz,  $\text{DMSO}-d_6$ )  $\delta$  163.7, 161.8, 161.5, 161.0, 159.7, 151.4, 150.1, 145.5, 140.3, 139.6, 134.4, 133.5, 131.9, 131.3, 130.6, 129.3, 128.7, 128.4, 127.5, 125.0, 124.0, 114.9, 104.9, 104.1. HRMS (MALDI-TOF,  $m/z$ ): calcd for  $\text{C}_{58}\text{H}_{38}\text{F}_4\text{N}_4\text{O}_2\text{P}_2\text{Ir}$   $[\text{M} - \text{PF}_6]^+$  1153.2035, found 1153.2028; calcd for  $\text{C}_{46}\text{H}_{30}\text{F}_4\text{N}_2\text{O}_2\text{P}_2\text{Ir}$   $[\text{M} - \text{PF}_6 - \text{phen}]^+$  973.1348, found 973.1061. Elem. anal. calcd (%) for  $\text{C}_{58}\text{H}_{38}\text{F}_{10}\text{IrN}_4\text{O}_2\text{P}_3$ : C, 53.67; H, 2.95; N, 4.32. Found: C, 53.50; H, 3.02; N, 4.34.

**POF2:** Yield 59%, yellow solid;  $^1\text{H}$  NMR (400 MHz,  $\text{DMSO}-d_6$ )  $\delta$  8.91 (d,  $J = 8.2$  Hz, 2H), 8.39 – 8.31 (m, 2H), 8.07 (d,  $J = 8.7$  Hz, 2H), 7.99 – 7.93 (m, 4H), 7.81 – 7.70 (m, 12H), 7.64 – 7.50 (m, 12H), 7.24 (t,  $J = 6.7$  Hz, 2H), 5.72 (dd,  $J = 9.6, 3.3$  Hz, 2H).  $^{13}\text{C}$  NMR (100 MHz,  $\text{DMSO}-d_6$ )  $\delta$  163.7, 162.3, 161.8, 161.5, 159.7, 154.9, 150.4, 149.9, 140.5, 134.4, 133.5, 131.9, 130.6, 130.5, 129.3, 129.0, 128.7, 128.6, 125.4, 124.1, 114.8, 104.8, 104.1. HRMS (MALDI-TOF,  $m/z$ ): calcd for  $\text{C}_{56}\text{H}_{38}\text{F}_4\text{N}_4\text{O}_2\text{P}_2\text{Ir}$   $[\text{M} - \text{PF}_6]^+$  1129.2035, found 1129.2035; calcd for  $\text{C}_{46}\text{H}_{30}\text{F}_4\text{N}_2\text{O}_2\text{P}_2\text{Ir}$   $[\text{M} - \text{PF}_6 - \text{bpy}]^+$  973.1348, found 973.1182. Elem. anal. calcd (%) for  $\text{C}_{56}\text{H}_{38}\text{F}_{10}\text{IrN}_4\text{O}_2\text{P}_3$ : C, 52.79; H, 3.01; N, 4.40. Found: C, 52.83; H, 3.38; N, 4.39.

**POF3:** Yield 56%, yellow-green solid;  $^1\text{H}$  NMR (400 MHz,  $\text{DMSO}-d_6$ )  $\delta$  8.73 (d,  $J = 8.4$  Hz, 2H), 8.15 (d,  $J = 7.5$  Hz, 2H), 8.09 (d,  $J = 8.7$  Hz, 2H), 7.96 (t,  $J = 7.7$  Hz, 2H), 7.79 – 7.69 (m, 10H), 7.65 – 7.58 (m, 6H), 7.57 – 7.50 (m, 8H), 7.24 (t,  $J = 6.6$  Hz, 2H), 5.74 – 5.70 (m, 2H), 2.35 (s, 6H).  $^{13}\text{C}$  NMR (100 MHz,  $\text{DMSO}-d_6$ )  $\delta$  163.6, 161.8, 161.5, 159.7, 152.6, 149.9, 140.9, 140.3, 139.2, 134.3, 133.4, 132.0, 129.0, 128.7, 128.6, 125.1, 124.3, 124.2, 124.0, 114.9, 104.6, 103.8, 18.2. HRMS (MALDI-TOF,  $m/z$ ): calcd for  $\text{C}_{58}\text{H}_{42}\text{F}_4\text{N}_4\text{O}_2\text{P}_2\text{Ir}$   $[\text{M} - \text{PF}_6]^+$  1157.2348, found 1157.2363; calcd for  $\text{C}_{46}\text{H}_{30}\text{F}_4\text{N}_2\text{O}_2\text{P}_2\text{Ir}$   $[\text{M} - \text{PF}_6 - \text{dMebpy}]^+$  973.1348, found 973.0884. Elem. anal. calcd (%) for  $\text{C}_{58}\text{H}_{42}\text{F}_{10}\text{IrN}_4\text{O}_2\text{P}_3$ : C, 53.50; H, 3.25; N, 4.30. Found: C, 52.90; H, 3.24; N, 4.36.

**POF4:** Yield 45%, lime green;  $^1\text{H}$  NMR (400 MHz,  $\text{DMSO}-d_6$ )  $\delta$  8.01 (d,  $J = 8.6$  Hz, 2H), 7.93 (t,  $J = 7.6$  Hz, 2H), 7.78 – 7.71 (m, 10H), 7.60 – 7.49 (m, 14H), 7.30 (t,  $J = 6.6$  Hz, 2H), 6.68 (s, 2H), 5.79 (dd,  $J = 9.8, 3.7$  Hz, 2H).  $^{13}\text{C}$  NMR (100 MHz,  $\text{DMSO}-d_6$ )  $\delta$  163.4, 162.4, 161.9, 161.4, 159.4, 149.5, 140.9, 139.5, 134.5, 133.5, 131.9, 130.5, 130.4, 129.5, 128.7, 128.6, 126.6, 124.5, 123.4, 122.4, 114.9, 103.6, 102.8. HRMS (MALDI-TOF,  $m/z$ ):

calcd for  $C_{52}H_{36}F_4N_6O_2P_2Ir [M - PF_6]^+$  1107.1940, found 1107.1923; calcd for  $C_{46}H_{30}F_4N_2O_2P_2Ir [M - PF_6 - biim]^+$  973.1348, found 973.1491. Elem. anal. calcd (%) for  $C_{52}H_{36}F_{10}IrN_6O_2P_3$ : C, 49.89; H, 2.90; N, 6.71. Found: C, 49.57; H, 3.31; N, 7.13.

**POF5:** Yield 41%, lime green;  $^1H$  NMR (400 MHz, DMSO- $d_6$ )  $\delta$  8.02 (d,  $J = 8.6$  Hz, 2H), 7.95 (t,  $J = 8.1$  Hz, 2H), 7.80 – 7.69 (m, 10H), 7.62 – 7.48 (m, 14H), 7.32 (t,  $J = 6.6$  Hz, 2H), 6.64 (d,  $J = 1.1$  Hz, 2H), 5.73 (dd,  $J = 9.8, 3.6$  Hz, 2H), 4.23 (s, 6H).  $^{13}C$  NMR (100 MHz, DMSO- $d_6$ )  $\delta$  163.3, 162.2, 161.6, 159.5, 149.7, 140.7, 139.7, 134.5, 133.7, 131.8, 130.5, 130.4, 129.4, 128.7, 128.6, 128.0, 126.7, 124.6, 123.4, 114.9, 103.8, 103.0, 37.9. HRMS (MALDI-TOF,  $m/z$ ): calcd for  $C_{54}H_{40}F_4N_6O_2P_2Ir [M - PF_6]^+$  1135.2253, found 1135.2231; calcd for  $C_{46}H_{30}F_4N_2O_2P_2Ir [M - PF_6 - dMebiim]^+$  973.1348, found 973.1061. Elem. anal. calcd (%) for  $C_{54}H_{40}F_{10}IrN_6O_2P_3$ : C, 50.67; H, 3.15; N, 6.57. Found: C, 50.97; H, 3.10; N, 6.37.

**POF6:** Yield 38%, green-yellow solid;  $^1H$  NMR (400 MHz, DMSO- $d_6$ )  $\delta$  8.27 (d,  $J = 5.7$  Hz, 2H), 8.07 (d,  $J = 8.7$  Hz, 2H), 7.99 (t,  $J = 7.9$  Hz, 2H), 7.82 – 7.72 (m, 10H), 7.65 – 7.57 (m, 4H), 7.56 – 7.49 (m, 8H), 7.37 (t,  $J = 6.7$  Hz, 2H), 7.22 – 7.08 (m, 10H), 6.98 (s, 2H), 5.81 (dd,  $J = 9.7, 3.0$  Hz, 2H).  $^{13}C$  NMR (100 MHz, DMSO- $d_6$ )  $\delta$  163.4, 162.1, 161.6, 161.3, 160.4, 159.5, 150.4, 140.0, 138.8, 135.7, 134.6, 133.8, 131.8, 130.6, 130.5, 129.6, 129.3, 128.7, 128.6, 128.1, 124.9, 124.6, 123.5, 115.2, 104.2, 103.4. HRMS (MALDI-TOF,  $m/z$ ): calcd for  $C_{46}H_{30}F_4N_2O_2P_2Ir [M - PF_6 - dPhbiim]^+$  973.1348; found 973.2037. Elem. anal. calcd (%) for  $C_{64}H_{44}F_{10}IrN_6O_2P_3$ : C, 54.74; H, 3.16; N, 5.98. Found: C, 54.33; H, 3.37; N, 5.64.

## Acknowledgements

The authors thank the financial support from the National Natural Science Foundation of China (21276043, 21421005), Dalian University of Technology (DUT, SYSWX201507), and Open Fund of Key Laboratory of Biotechnology and Bioresources Utilization (Dalian Minzu University, KF2015002), State Ethnic Affairs Commission & Ministry of Education. We thank Prof. Jiuyan Li and Prof. Jiangli Fan at DUT, for valuable discussions on this work. Many thanks also to Prof. Jianzhang Zhao at DUT for his assistance on the theoretical calculations.

## References

- W. Y. Wong and C. L. Ho, *Coord. Chem. Rev.*, 2009, **253**, 1709-1758.
- Y. You and W. Nam, *Chem. Soc. Rev.*, 2012, **41**, 7061-7084.
- J. R. Chen, X. Q. Hu, L. Q. Lu and W. J. Xiao, *Chem. Soc. Rev.*, 2016, **45**, 2044-2056.
- K. W. Lo and K. S. Tso, *Inorg. Chem. Front.*, 2015, **2**, 510-524.
- S. Ladouceur and E. Zysman-Colman, *Eur. J. Inorg. Chem.*, 2013, 2972-2972.
- C. L. Ho, Y. Bing, B. Zhang, K. L. Wong, W. Y. Wong, Z. Xie, L. Wang and Z. Lin, *J. Organomet. Chem.*, 2013, **730**, 144-155.
- R. D. Costa, E. Ortí, H. J. Bolink, F. Monti, G. Accorsi and N. Armaroli, *Angew. Chem., Int. Ed.*, 2012, **51**, 8178-8211.
- X. Yang, X. Xu, J. S. Dang, G. Zhou, C. L. Ho and W. Y. Wong, *Inorg. Chem.*, 2016, **55**, 1720-1727.
- Y. You and S. Y. Park, *Dalton Trans.*, 2009, **8**, 1267-1282.
- Y. Chi and P. Chou, *Chem. Soc. Rev.*, 2010, **39**, 1638-1639. DOI: 10.1039/C9TC004732G
- C. L. Ho and W. Y. Wong, *New J. Chem.*, 2013, **37**, 1665-1683.
- C. Adachi, R. C. Kwong, P. Djurovich, V. Adamovich, M. A. Baldo, M. E. Thompson and S. R. Forrest, *Appl. Phys. Lett.*, 2001, **79**, 2082-2084.
- C. F. Chang, Y. M. Cheng, Y. Chi, Y. C. Chiu, C. C. Lin, G. H. Lee, P. T. Chou, C. C. Chen, C. H. Chang and C. C. Wu, *Angew. Chem., Int. Ed.*, 2008, **47**, 4542-4545.
- Y. Chiu, Y. Chi, J. Hung, Y. Cheng, Y. Yu, M. Chung, G. Lee, P. Chou, C. Chen and C. Wu, *ACS Appl. Mater. Interfaces*, 2009, **1**, 433.
- J. B. Kim, S. H. Han, K. Yang, S. K. Kwon, J. J. Kim and Y. H. Kim, *Chem. Commun.*, 2015, **51**, 58-61.
- M. Marín-Suárez, B. F. E. Curchod, I. Tavernelli, U. Rothlisberger, R. Scopelliti, I. Jung, D. D. Censo, M. Grätzel and A. Fernández-Gutiérrez, *Chem. Mater.*, 2012, **24**, 2330-2338.
- S. Lee, S. O. Kim, H. Shin, H. J. Yun, K. Yang, S. K. Kwon, J. J. Kim and Y. H. Kim, *J. Am. Chem. Soc.*, 2013, **135**, 14321-14328.
- T. Kim, J. Lee, U. L. Sang and H. L. Min, *Organometallics*, 2015, **34**, 3455-3458.
- D. Ma, L. Duan, Y. Wei, L. He, L. Wang and Y. Qiu, *Chem. Commun.*, 2014, **50**, 530-532.
- F. Hsu, C. Chien, C. Shu, C. Lai, C. Hsieh, K. Wang and P. Chou, *Adv. Funct. Mater.*, 2009, **19**, 2834-2843.
- S. O. Jeon and J. Y. Lee, *J. Mater. Chem.*, 2012, **22**, 4233-4243.
- X. Yang, G. Zhou and W. Y. Wong, *Chem. Soc. Rev.*, 2015, **44**, 8484-8575.
- G. Zhou, C. L. Ho, W. Y. Wong, Q. Wang, D. Ma, L. Wang, Z. Lin, T. B. Marder and A. Beeby, *Adv. Funct. Mater.*, 2008, **18**, 499-511.
- G. Zhou, C. Ho, W. Wong, D. Ma, L. Wang and Z. Lin, *Chem. - Asian J.*, 2008, **3**, 1830-1841.
- L. Deng, T. Zhang, R. Wang and J. Li, *J. Mater. Chem.*, 2012, **22**, 15910-15918.
- M. Zhu, Y. Li, J. Miao, B. Jiang, C. Yang, H. Wu, J. Qin and Y. Cao, *Org. Electron.*, 2014, **15**, 1598-1606.
- L. Wang, Y. Wu, G. G. Shan, Y. Geng, J. Z. Zhang, D. M. Wang, G. C. Yang and Z. M. Su, *J. Mater. Chem. C*, 2014, **2**, 2859-2868.
- C. Fan, Y. Li, C. Yang, H. Wu, J. Qin and Y. Cao, *Chem. Mater.*, 2012, **24**, 4581-4587.
- H. Yun, K. Kim, S. Kang, J. Kim and Y. Kim, *Isr. J. Chem.*, 2014, **54**, 993-998.
- Y. Si, S. Zhang, N. Qu, G. Luan and Z. Wu, *New J. Chem.*, 2015, **39**, 4147-4153.
- L. He, J. Qiao, L. Duan, G. Dong, D. Zhang, L. Wang and Y. Qiu, *Adv. Funct. Mater.*, 2009, **19**, 2950-2960.
- F. Sguerra, R. Marion, G. H. V. Bertrand, R. Coulon, É. Sauvageot, R. Daniellou, J. L. Renaud, S. Gaillard and M. Hamel, *J. Mater. Chem.*, 2014, **2**, 6125-6133.
- J. I. Goldsmith, W. R. Hudson, M. S. Lowry, T. H. Anderson and S. Bernhard, *J. Am. Chem. Soc.*, 2005, **127**, 7502-7510.
- D. Tordera, A. M. Bünzli, A. Pertegás, J. M. Junquera-Hernández, E. C. Constable, J. A. Zampese, C. E. Housecroft, E. Ortí and H. J. Bolink, *Chem. - Eur. J.*, 2013, **19**, 8597-8609.
- Y. Zhou, J. Jia, X. Wang, W. Guo, Z. Wu and N. Xu, *Chem. - Eur. J.*, 2016, **22**, 16796-16800.
- A. F. Henwood, S. Evariste, A. M. Slawin and E. Zysman-Colman, *Faraday Discuss.*, 2014, **174**, 165-182.
- M. Mydlak, C. Bizzarri, D. Hartmann, W. Sarfert, G. Schmid and L. D. Cola, *Adv. Funct. Mater.*, 2010, **20**, 1812-1820.
- M. K. Itokazu, A. S. Polo and N. Y. M. Iha, *J. Photochem. Photobiol., A*, 2003, **160**, 27-32.

- 39 F. Sguerra, R. Marion, G. Bertrand, R. Coulon, É. Sauvageot, R. Daniellou, J. L. Renaud, S. Gaillard and M. Hamel, *J. Mater. Chem. C*, 2014, **2**, 6125-6133.
- 40 H. F. Chen, W. Y. Hung, S. W. Chen, T. C. Wang, S. W. Lin, S. H. Chou, C. T. Liao, H. C. Su, H. A. Pan and P. T. Chou, *Inorg. Chem.*, 2012, **51**, 12114-12121.
- 41 F. Zhang, D. Ma, L. Duan, J. Qiao, G. Dong, L. Wang and Y. Qiu, *Inorg. Chem.*, 2014, **53**, 6596-6606.
- 42 N. M. Shavaleev, G. Xie, S. Varghese, D. B. Cordes, A. M. Slawin, C. Momblona, E. Ortí, H. J. Bolink, I. D. Samuel and E. Zysman-Colman, *Inorg. Chem.*, 2015, **54**, 5907-5914.
- 43 Y. You, H. S. Huh, K. S. Kim, S. W. Lee, D. Kim and S. Y. Park, *Chem. Commun.*, 2008, **34**, 3998-4000.
- 44 G. Shan, D. Zhu, H. Li, P. Li, Z. Su and Y. Liao, *Dalton Trans.*, 2011, **40**, 2947-2953.
- 45 V. Sathish, A. Ramdass, P. Thanasekaran, K. Lu and S. Rajagopal, *J. Photochem. Photobiol. C*, 2015, **23**, 25-44.
- 46 X. D. Wang and O. S. Wolfbeis, *Chem. Soc. Rev.*, 2014, **43**, 3666-3761.
- 47 C. S. K. Mak, D. Pentlehner, M. Stich, O. S. Wolfbeis, W. K. Chan and H. Yersin, *Chem. Mater.*, 2009, **21**, 2173-2175.
- 48 E. M. Boreham, L. Jones, A. N. Swinburne, M. Blancharddesce, V. Hugues, C. Terryn, F. Miomandre, G. Lemerrier and L. S. Natrajan, *Dalton Trans.*, 2015, **44**, 16127-16135.
- 49 C. Liu, X. Lv, Y. Xing and J. Qiu, *J. Mater. Chem. C*, 2015, **3**, 8010-8017.
- 50 C. Liu, H. Yu, X. Rao, X. Lv, Z. Jin and J. Qiu, *Dyes Pigm.*, 2017, **136**, 641-647.
- 51 C. Liu, H. Yu, Y. Xing, Z. Gao and Z. Jin, *Dalton Trans.*, 2016, **45**, 734-741.
- 52 W. Xu, R. C. McDonough III, B. Langsdorf, J. Demas and B. DeGraff, *Anal. Chem.*, 1994, **66**, 4133-4141.
- 53 K. A. McGee and K. R. Mann, *J. Am. Chem. Soc.*, 2009, **131**, 1896-1902.
- 54 Y. Xiong, Z. Ye, J. Xu, Y. Zhu, C. Chen and Y. Guan, *Analyst*, 2013, **138**, 1819-1827.
- 55 M. J. Frisch, G. Trucks, H. Schlegel, G. Scuseria, M. Robb, J. Cheeseman, G. Scalmani, V. Barone, B. Mennucci and G. Petersson, *Gaussian Inc., Wallingford, CT*, 2009.

View Article Online  
DOI: 10.1039/C6TC04732G

# Effect of ancillary ligands on the properties of diphenylphosphoryl-substituted cationic Ir(III) complexes

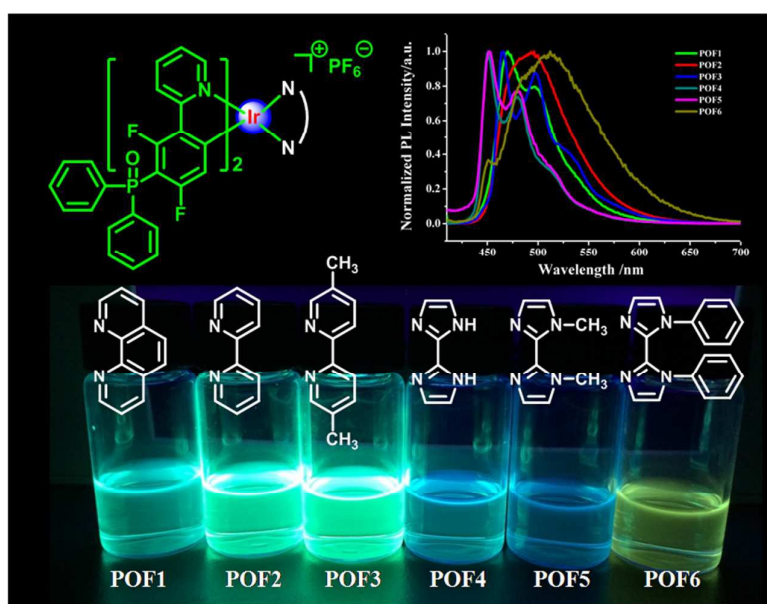
Hongcui Yu, Chun Liu\*, Zhenni Yu, Liyan Zhang and Jinghai Xiu\*

[\*]Corresponding Author

State Key Laboratory of Fine Chemicals, Dalian University of Technology, Linggong Road 2, Dalian 116024, China.

Tel.: +86-411-84986182.

E-mails: cliu@dlut.edu.cn; xiujh@dlut.edu.cn



A new class of greenish-blue to blue emitting diphenylphosphoryl-substituted cationic cyclometalated Ir(III) complexes (**POF1-POF6**) with different N<sup>N</sup> ancillary ligands are reported.